

## Strong octupole and dipole collectivity in $^{96}\text{Zr}$ : Indication for octupole instability in the $A = 100$ mass region

H. Mach,<sup>(1-3)</sup> S. Ćwiok,<sup>(4,5)</sup> W. Nazarewicz,<sup>(4,6)</sup> B. Fogelberg,<sup>(1)</sup>  
M. Moszyński,<sup>(3,7)</sup> J. Winger,<sup>(3,8)\*</sup> and R. L. Gill<sup>(3)</sup>

<sup>(1)</sup>The Studsvik Neutron Research Laboratory, S-61182, Nyköping, Sweden

<sup>(2)</sup>Institut für Kernphysik, Kernforschungsanlage Jülich, D-5170 Jülich, Federal Republic of Germany

<sup>(3)</sup>Brookhaven National Laboratory, Upton, New York 11973

<sup>(4)</sup>Institute of Physics, Warsaw University of Technology, PL 00-662, Warsaw, Poland

<sup>(5)</sup>Gesellschaft für Schwerionenforschung Darmstadt, D-6100 Darmstadt 11, Federal Republic of Germany

<sup>(6)</sup>Institute of Theoretical Physics, Warsaw University, PL-00662, Warsaw, Poland

<sup>(7)</sup>Institute for Nuclear Studies, PL 05-400, Świerk-Otwock, Poland

<sup>(8)</sup>Ames Laboratory, Iowa State University, Ames, Iowa 50011

(Received 12 February 1990)

A half-life of  $T_{1/2} = 50(7)$  ps was measured for the  $3_1^-$  level in  $^{96}\text{Zr}$ . The deduced  $B(E3)$  rate of 65(10) W.u. makes this  $3_1^- \rightarrow 0_1^+$  transition the fastest known. The results interpreted in terms of the random phase approximation and a deformed shell model suggest octupole instability around  $^{96}\text{Zr}$ .

The systematics of the  $B(E3)$  rates in the  $A = 100$  region show<sup>1</sup> a strong enhancement at  $^{96}\text{Zr}$ . Mutually reinforcing particle-hole excitations of the proton  $2p_{3/2} \rightarrow 1g_{9/2}$  and neutron  $2d_{5/2} \rightarrow 1h_{11/2}$  across the  $Z = 40$  and  $N = 56$  gaps, respectively, could produce large octupole collectivity exceeding even that for  $^{40}\text{Ca}$  and  $^{208}\text{Pb}$ .<sup>2</sup> The  $B(E3; 3_1^- \rightarrow 0_1^+)$  in  $^{96}\text{Zr}$  obtained<sup>1</sup> from a lifetime measurement,  $B(E3) = 39 \pm_{13}^{49}$  W.u., has a large uncertainty. Similarly, the  $B(E3)$  value of 48(16) W.u. deduced from the angular distributions of inelastically scattered protons<sup>3</sup> is strongly model dependent, and therefore is less reliable than the traditional methods of Coulomb excitation and lifetime measurements. However, both results imply an exceptionally strong  $B(E3)$  rate in  $^{96}\text{Zr}$ . Moreover, calculations within the *spdf* boson version of the interacting boson model predict<sup>4</sup> an enhanced  $B(E3)$  rate of about 36 W.u. It is the purpose of this paper to report a precise lifetime measurement for the  $3_1^-$  level in  $^{96}\text{Zr}$  and to interpret the exceptionally strong  $B(E1)$  and  $B(E3)$  rates in terms of the random phase approximation (RPA) and a deformed shell model.

Lifetimes of the  $^{96}\text{Zr}$  levels (populated in the low spin  $\beta^-$  decay of  $^{96}\text{Y}$ ) were measured at the fission product mass separator TRISTAN at Brookhaven National Laboratory. Measurements were performed in the daughter port configuration<sup>5</sup> using a recently developed  $\beta$ - $\gamma$ - $\gamma$  fast timing method.<sup>5-8</sup> The radioactive source, which was brought sequentially on tape from the deposition port to the counting station, contained also the  $^{96}\text{Sr}$  and  $^{95}\text{Sr}$  isotopes (the latter from the  $\beta$ -delayed neutron decay of  $^{96}\text{Rb}$ ). Lifetime information was derived from  $\beta$ - $\gamma$  delayed coincidences in fast timing detectors (a thin NE111A plastic for  $\beta$  rays and a small  $\text{BaF}_2$  crystal for  $\gamma$  transitions). The  $\Delta E$   $\beta$  detector provided a  $\beta$  response almost independent of the feeding  $\beta$ -ray energy while an additional  $\gamma$  coincidence with a Ge detector was used to select the desired decay path.

Lifetimes were obtained from the centroid shift technique. In the case of a direct  $\beta$  feeding to a level of interest the mean life ( $T_{1/2}/\ln 2$ ) is the difference between the centroid of the delayed time spectrum and the prompt centroid for the same  $E_\gamma$ . When the level of interest is fed by a  $\gamma$  ray from a higher level the mean life of interest is the difference between the centroid shift of the spectrum gated by the deexciting  $\gamma$  ray and the centroid shift of the spectrum gated by the feeding  $\gamma$  transition.

$T_{1/2} = 50(7)$  ps measured for the  $3_1^-$  1897.1-keV level is the average of two results. The first one,  $T_{1/2} = 58(11)$  ps (see Fig. 1) is the difference between the centroids of the 475–1750 and 328–1750 time spectra. (In our convention the 475–1750 spectrum was sorted with a 475-keV transition selected in the Ge detector and the 1750-keV transition in the  $\text{BaF}_2$  crystal.) Since both the 475- and 328-keV transitions deexcite the same level, and identical 1750-keV energy gates were selected in the  $\text{BaF}_2$  crystal, no corrections (except for the usual background subtraction in each detector) nor any knowledge of the prompt were needed in the analysis. The second result was deduced from the centroid shift [ $\tau_1 = 78(11)$  ps] of the 147–1750 time distribution from the prompt and corrected for the time delay [ $\tau_2 = 13(6)$  ps] introduced by  $\gamma$  cascades from higher-lying levels, to yield  $T_{1/2} = \ln 2(\tau_1 - \tau_2) = 45(9)$  ps. The position of the prompt was obtained following a procedure discussed next.

Using a set of calibration lines, the shape of the prompt curve was determined for the  $\text{BaF}_2$  detector as a function of  $\gamma$  energy for  $0.4 \leq E_\gamma \leq 2.8$  MeV. To account for electronics drifts between the calibration and Zr measurements, the prompt calibration is usually obtained by shifting this relative curve by a constant to overlap with points absolutely calibrated and internal to the decay of interest. However, due to a low coincidence rate observed for the low-spin  $^{96}\text{Y} \rightarrow \text{Zr}$  decay (only 1% of the  $\beta$  feeding goes to excited states with  $E_\gamma \geq 2$  MeV, see Fig. 2) it was not

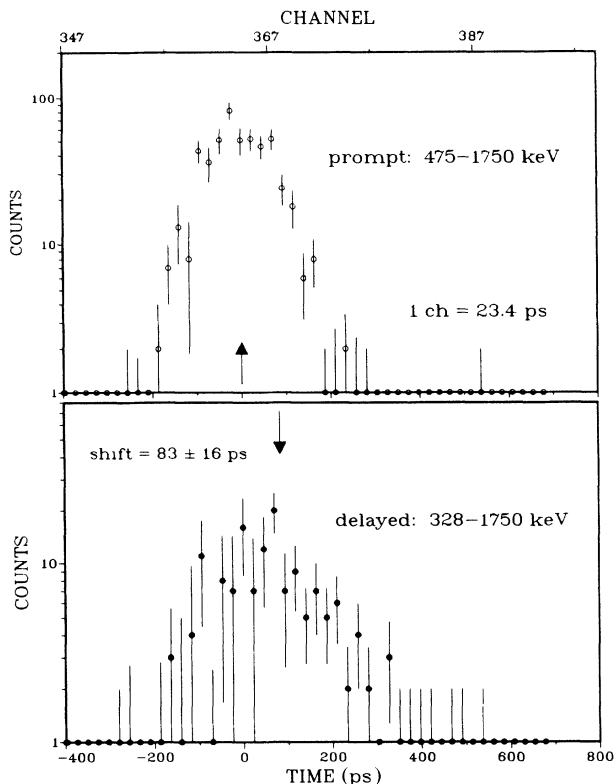


FIG. 1. Time spectra used to deduce the lifetime of the 1897-keV state. Start signals  $\beta^-$  particles and stop signals 1750-keV  $\gamma$  rays. Spectra *a* and *b* were gated by 475- and 328-keV  $\gamma$  rays in a Ge detector, respectively. A shift of  $\tau = 83(16)$  ps between their centroids (indicated by arrows) is equal to the meanlife of the  $3_1^+$  level [ $T_{1/2} = 58(11)$  ps].

possible to normalize the  $^{96}\text{Y} \rightarrow \text{Zr}$  prompt to the usual “internal calibration region” at 2–3 MeV.<sup>5,6</sup> Thus, a position of the  $^{96}\text{Y} \rightarrow \text{Zr}$  prompt was obtained by relating it to the position of the well defined  $^{95}\text{Sr} \rightarrow \text{Y}$  prompt. In the first approach the  $2_1^+ \rightarrow 0_1^+$  transition in  $^{96}\text{Zr}$  deexciting the 1750.4-keV level [with  $T_{1/2} = 0.3(1)$  ps (Ref. 11), see Fig. 2] served as an internal calibration point, from which we deduce a shift of 13(11) ps between the  $^{96}\text{Y} \rightarrow \text{Zr}$  and the  $^{95}\text{Sr} \rightarrow \text{Y}$  prompt curves. This shift was also deduced from the prompt curves for the  $\beta^-$  decay of  $^{95,96}\text{Sr} \rightarrow \text{Y}$  measured concurrently with the  $^{96}\text{Y} \rightarrow \text{Zr}$  decay. With steady counting rates the  $^{96}\text{Y} \rightarrow \text{Zr}$  and  $^{95}\text{Sr} \rightarrow \text{Y}$  prompt curves would differ by only a few picoseconds. However, the measurement required the use of a moving tape to suppress the short-lived decay of  $^{96}\text{Rb}$ , and thus, the source strength varies from strong (at the beginning of the counting period) to weak (at the end of the counting period). The variation in the counting rate which was as much as 130000 counts/s in the  $\beta$  detector caused periodic fluctuations in the performance of the electronics, and resulted in a degraded time resolution. Typically, a full width at half maximum equals 160 ps at 1.3 MeV was achieved. Moreover, a shift of 22 ps between the prompt curves for the  $^{96}\text{Sr} \rightarrow \text{Y}$  and  $^{95}\text{Sr} \rightarrow \text{Y}$  decays was observed. The shape of the prompt curve was found to be the same for both decays and thus, within the experimental precision, it was not affected by the rate

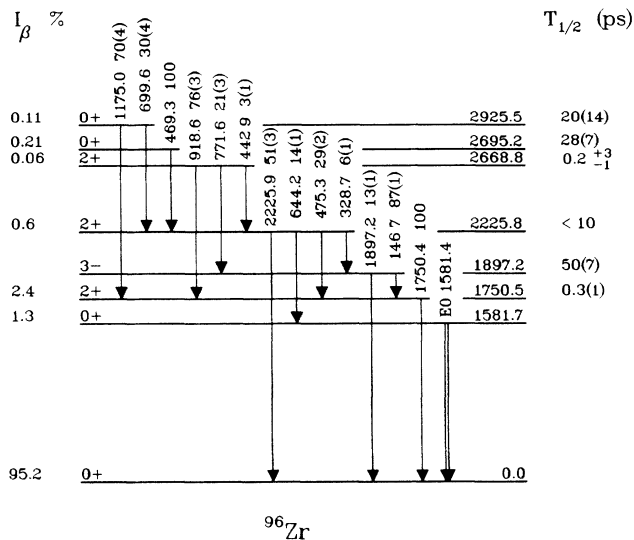


FIG. 2. A partial level scheme for the  $0^- \text{ } ^{96}\text{Y} \rightarrow \text{ } ^{96}\text{Zr}$  decay.  $I_\beta$ , energy levels and branching ratios are taken from Refs. 9 and 10. The half-lives indicated on the right of each level are from this work except for the 1750.5- and the 2668.8-keV levels which are taken from Refs. 11 and 12, respectively.

fluctuations. Since the rate observed for the decay of  $^{96}\text{Y} \rightarrow \text{Zr}$  was intermediate to that for  $^{95,96}\text{Sr} \rightarrow \text{Y}$ , its prompt curve should lie between the other two. Thus the prompt of  $^{96}\text{Y} \rightarrow \text{Zr}$  was defined at 11(11) ps above the prompt of  $^{95}\text{Sr} \rightarrow \text{Y}$ . An average value of 12(9) ps was adopted for the analysis.

The lifetimes are summarized in Fig. 2. Using  $T_{1/2} = 50(7)$  and the branching ratios from Ref. 10 we deduce the  $B(E3; 3_1^- \rightarrow 0_1^+)$  of 65(10) W.u. which is consistent with previous results of  $39^{+49}_{-5}$  W.u. (Ref. 1) and 48(16) W.u. (Ref. 3). The most significant outcome of the present investigation is the establishment of the E3 transition in  $^{96}\text{Zr}$  as the fastest known. This can be seen from the systematics of the  $B(E3)$  rates given by Spear.<sup>13</sup> For doubly magic  $^{40}\text{Ca}$  and  $^{208}\text{Pb}$  the  $B(E3)$  rates are 31(3) and 34.0(5) W.u., respectively. For the nearby  $^{90}\text{Zr}$  and  $^{98}\text{Mo}$  the rates are 32(1) and 33(3) W.u., respectively. Slightly higher values of  $\sim 40$  W.u. are seen in the Nd-Gd region with  $B(E3)$  of 26(3) W.u. ( $^{146}\text{Nd}$ ), 44(9) W.u. ( $^{148}\text{Nd}$ ), 39(3) W.u. ( $^{148}\text{Sm}$ ), and 33(3) W.u. ( $^{150}\text{Sm}$ ), as well as 37(2) and 52(17) W.u. for  $^{146,152}\text{Gd}$ , respectively. In the transuranium region the strongest  $B(E3)$  of 35(2) W.u. is observed for  $^{226}\text{Ra}$ . The latter values are related to the presence of stable octupole deformation that has been established in the heavy-Ba and light-actinide regions.

The exceptionally high  $B(E3)$  rate challenges the theoretical interpretation. Let us first analyze the structure of the  $3_1^-$  state within the RPA, which is expected to work well if the octupole vibrations are *harmonic*. Within RPA it is easy to see why the conditions for the  $B(E3)$  rate are particularly optimal in  $^{96}\text{Zr}$ . At  $Z = 40$  and  $N = 56$  the  $\pi p_{3/2}$ ,  $\nu g_{9/2}$ , and  $\nu d_{5/2}$  subshells are filled, while the corresponding  $\pi g_{9/2}$  and  $\nu h_{11/2}$  subshells are empty. By the same argument (see also Ref. 1) the  $B(E3)$  rates in  $^{90}\text{Zr}$  [with no  $\nu(d_{5/2} \rightarrow h_{11/2})$  contribu-

tion] and in  $^{98}\text{Mo}$  [with a partially blocked  $\pi(p_{3/2} \rightarrow g_{9/2})$  contribution due to a partial filling of the  $\pi g_{9/2}$  orbit] are expected and observed<sup>13</sup> to be much lower. In our simple analysis we assume that the ground state of  $^{96}\text{Zr}$  is spherical due to its semimagnetic character. For the same reason we neglect pairing correlations as they are expected to be seriously quenched because of the large  $Z=40$  and  $N=56$  gaps in the single-particle spectrum. The octupole-octupole isoscalar force was used for the residual interaction. The reduced  $M(E3, 3^- \rightarrow \text{g.s.})$  transition matrix element for the lowest collective  $3^-$  excitation was then calculated according to Refs. 14 and 15.

In this simple calculation of the  $B(E3)$  rate, we did not solve the RPA secular equations to determine the energy of the lowest collective one phonon state,  $\Omega$ , but rather took the experimental value of  $\Omega = 1.897$  MeV. Furthermore, only the four leading particle-hole ( $p$ - $h$ ) components, i.e.,  $\nu(h_{11/2} \rightarrow d_{5/2})$  ( $\Delta e = 2.8$  MeV),  $n(h_{11/2} \rightarrow g_{9/2})$  ( $\Delta e = 8.3$  MeV),  $\pi(g_{9/2} \rightarrow p_{3/2})$  ( $\Delta e = 2.8$  MeV), and  $\pi(g_{9/2} \rightarrow f_{5/2})$  ( $\Delta e = 3.7$  MeV) have been considered. The energies  $\Delta e$  of  $p$ - $h$  excitations were taken according to Refs. 15 and 16. To calculate radial matrix elements we employed the harmonic oscillator wave functions with the oscillator frequency from the Nilsson model,  $\hbar\omega_0 = 41A^{-1/3}[1 \pm (N-Z)/3A]$  (where the plus sign holds for neutrons and the minus sign for protons). In more realistic calculations the number of possible  $p$ - $h$  excitations contributing to the collective transition is very large, and in order to account for them, effective charges are needed. With the effective charges taken from Ref. 16 as  $e_n^{\text{eff}} = 0.8e$  and  $e_p^{\text{eff}} = 1.2e$  the calculated  $B(E3)$  rate is 19 W.u. Agreement with the data would be obtained if drastically larger effective charges,  $e_p^{\text{eff}} = e_n^{\text{eff}} = 1.6e$ , were used [ $B(E3) = 55$  W.u.]. As expected, the dominant component of the  $B(E3)$  rate comes from the non-spin-flip (stretched)  $\pi(p_{3/2} \rightarrow g_{9/2})$  and  $\nu(d_{5/2} \rightarrow h_{11/2})$  transitions. The stretched  $\nu(g_{9/2} \rightarrow h_{11/2})$  excitation has a large transition matrix element, but because of the large energy denominator its contribution to the  $B(E3)$  is only about 15%.

In the global RPA analysis of octupole states by Veje<sup>15</sup>  $\Omega = 1.62$  MeV and  $B(E3) = 25$  W.u. were obtained for  $^{96}\text{Zr}$ . Clearly, it is very difficult to obtain a consistent description of both the  $3_1^-$  excitation energy and the value of  $B(E3)$  rate in  $^{96}\text{Zr}$  using the RPA formalism with standard parameters. One can thus conclude that the unusually strong octupole collectivity of  $^{96}\text{Zr}$  is probably not consistent with simple harmonic octupole vibrations and some other mechanism should be present.

A possible scenario is offered by deformed shell model. The Woods-Saxon model<sup>2,17</sup> has predicted a pronounced octupole softness at near-spherical configurations in many nuclei in the  $A=100$  mass region. This result is consistent with the previous calculations<sup>18</sup> which used the RPA method with self-consistent wave functions obtained from the Skyrme-III effective force. For  $^{96}\text{Zr}$  the RPA solution turned out to be unstable, characteristic of a transition from the spherical to the deformed limit. Of course, in the region of shape transition *the whole RPA formalism breaks down* and this probably explains why we could not reproduce the  $B(E3)$  rate without introducing drastically

higher effective charges.

In order to test the concept of octupole instability in  $^{96}\text{Zr}$ , shell correction calculations with the same Woods-Saxon potential and monopole pairing interaction as in Refs. 2 and 17 were performed. In contrast to Refs. 2 and 17, pairing energy was computed by employing the approximate particle number projection before variation. The total energy of a nucleus was minimized in four-dimensional deformation space:  $\beta_2, \beta_3, \beta_4, \beta_5$  (see also Refs. 19 and 20). Figure 3 shows the calculated potential-energy surface (PES) for  $^{96}\text{Zr}$  in the  $(\beta_2, \beta_3)$  plane (at each grid point the total energy has been minimized with respect to  $\beta_4$  and  $\beta_5$ ). It is well known<sup>2</sup> that the calculated PES around  $^{96}\text{Zr}$  is very sensitive to the choice of potential parameters. Therefore, we decided to perform calculations using two versions of the Woods-Saxon spin-orbit parameters. In Fig. 3(a), the same stan-

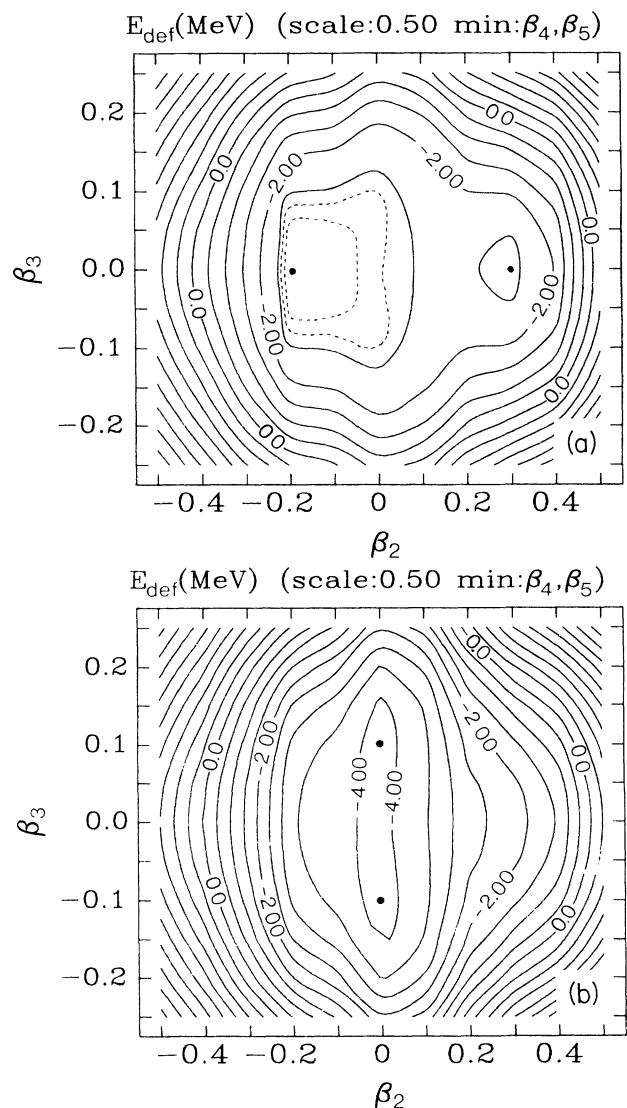


FIG. 3. Total energy surface in the  $(\beta_2, \beta_3)$  plane for  $^{96}\text{Zr}$  obtained with the Woods-Saxon potential including pairing. Two variants of spin-orbit parameters have been used, see text. The contour lines are 250 keV apart.

standard set of Woods-Saxon parameters was used, variant in Fig. 3(a), as was employed in Ref. 17. In this case, the PES for  $^{96}\text{Zr}$  is calculated to be extremely shallow in both the  $\beta_2$  and  $\beta_3$  directions. The actual minimum corresponds to an oblate deformation of  $\beta_2 \approx -0.2$ . It is clear that in this case the concept of a well-defined shape breaks down and one should rather expect a very complex *anharmonic* quadrupole-octupole motion. A weak secondary minimum can also be seen at  $\beta_2 \approx 0.28$ . With increasing neutron number this configuration becomes a ground state in heavier Zr isotopes. In Fig. 3(b), we employed the modified Woods-Saxon parameters of Ref. 2 (see Fig. 3 therein) that reproduced the shape transition between  $^{96}\text{Zr}$  and  $^{100}\text{Zr}$ , variant in Fig. 3(b). The new parameters slightly increase the spherical  $Z=40$  and  $N=56$  gaps and, therefore, stabilize the spherical configuration as seen in Fig. 3(b) [note that the modified single-particle levels of variant in Fig. 3(b) agree well with those used in Ref. 15]. The corresponding PES still remains quadrupole-soft especially towards oblate distortions. As compared to the variant in Fig. 3(a) the softness towards octupole deformation increases and, in fact, the calculated equilibrium shape is now reflection asymmetric with  $\beta_3 \approx 0.1$ .

The calculations for  $^{98}\text{Zr}$  using the variant in Fig. 3(b) also indicate strong octupole instability with  $\beta_3 = 0.13$  in its ground-state spherical configuration. The excited deformed minimum with  $\beta_2 \approx 0.3$  is reflection symmetric. The ground state of  $^{100}\text{Zr}$  is strongly deformed with  $\beta_2 \approx 0.34$ , which can be nicely compared to the experimental value of 0.34(1).<sup>7</sup> However, the secondary oblate minimum ( $\beta_2 \approx -0.17$ ) is again octupole unstable ( $\beta_3 \approx 0.05$ ). The variant in Fig. 3(a) gives a very similar answer. It would be very interesting to measure the

$B(E3)$  rates in  $^{98,100}\text{Zr}$  to see whether a similar enhancement in octupole strength also takes place in these nuclei. In all the mean-field calculations we neglected the  $\mu \neq 0$  components of the octupole tensor, which should certainly play a role at nearly spherical shapes. However, the inclusion of nonaxial components can only reinforce the instability.

Another feature of the  $3_1^-$  level is an exceptionally fast  $B(E1)$  rate of 0.0018(3) W.u. for the  $3_1^- \rightarrow 2_1^+$  transition. The large  $B(E3)$  and  $B(E1)$  rates in  $^{96}\text{Zr}$  are comparable to those for nuclei in the heavy Sm-Ba (Refs. 13 and 21) and the Ra-Th regions<sup>22</sup> which are expected to be octupole unstable<sup>17</sup> [e.g.,  $B(E1) = 0.0028(7)$  W.u. was observed<sup>21</sup> for  $^{144}\text{Ba}$  and explained<sup>23</sup> in terms of octupole deformation].

In summary, the lifetime of  $T_{1/2} = 50(7)$  ps was measured for the  $3_1^-$  state in  $^{96}\text{Zr}$ . The established fastest known  $B(E3; 3_1^- \rightarrow 0_1^+)$  rate of 65(10) W.u. has been interpreted in terms of octupole instability in  $^{96}\text{Zr}$  and suggests very strong octupole anharmonicities in this nucleus and its neighbors. Recent calculations<sup>2</sup> point toward the key role played by the  $\nu h_{11/2}$  orbit on the structure of heavy Zr nuclei. Indeed, the importance of this orbit may provide the unifying ingredient responsible for the extraordinary enhancement of the octupole collectivity in  $^{96}\text{Zr}$  and strong quadrupole collectivity in  $^{100}\text{Zr}$ .<sup>7</sup>

Discussions with E. Warburton, K. Sistemich, and G. Molnár are gratefully acknowledged. This work has been supported in part by the Swedish Natural Science Research Council, the Polish Ministry of National Education under Contract No. CPBP01.09 and the U.S. Department of Energy under Contracts No. DE-AC02-76CH00016 and No. W-7405-82.

\*Present address: National Superconducting Cyclotron Laboratory, Michigan State University, East Lansing, MI 48824-1321.  
<sup>1</sup>G. Molnár, H. Ohm, G. Lhersonneau, and K. Sistemich, *Z. Phys. A* **331**, 97 (1988).  
<sup>2</sup>W. Nazarewicz and T. Werner, in *Proceedings of the International Workshop on Nuclear Structure of the Zirconium Region, Bad Honnef, Federal Republic of Germany, 1988*, edited by J. Eberth, R. A. Meyer, and K. Sistemich (Springer-Verlag, Berlin, 1988), p. 277.  
<sup>3</sup>M. M. Stautberg, R. R. Johnson, J. J. Kraushaar, and B. W. Ridley, *Nucl. Phys. A* **104**, 67 (1967).  
<sup>4</sup>D. F. Kusnezov, E. A. Henry, and R. A. Meyer, *Phys. Lett. B* **228**, 11 (1989).  
<sup>5</sup>H. Mach, R. L. Gill, and M. Moszyński, *Nucl. Instrum. Methods Phys. Res. Sect. A* **280**, 49 (1989).  
<sup>6</sup>M. Moszyński and H. Mach, *Nucl. Instrum. Methods Phys. Res. Sect. A* **277**, 407 (1989).  
<sup>7</sup>H. Mach, M. Moszyński, R. L. Gill, F. K. Wohn, J. A. Winger, J. C. Hill, G. Molnár, and K. Sistemich, *Phys. Lett. B* **230**, 21 (1989).  
<sup>8</sup>H. Mach *et al.*, *Phys. Rev. Lett.* **63**, 143 (1989).  
<sup>9</sup>H. Mach, G. Molnár, S. W. Yates, R. L. Gill, A. Aprahamian, and R. A. Meyer, *Phys. Rev. C* **37**, 254 (1988).  
<sup>10</sup>G. Molnár *et al.*, *Nucl. Phys. A* **500**, 43 (1989).  
<sup>11</sup>H.-W. Mueller, *Nucl. Data Sheets* **35**, 281 (1982).  
<sup>12</sup>T. Belgya, G. Molnár, B. Fazekas, Á. Veres, R. A. Gatenby,

and S. W. Yates, *Nucl. Phys. A* **500**, 77 (1989).  
<sup>13</sup>R. H. Spear, *At. Data Nucl. Data Tables* **42**, 55 (1989).  
<sup>14</sup>V. G. Soloviov, *Theory of Complex Nuclei* (Nauka, Moscow, 1971).  
<sup>15</sup>C. J. Veje, *Kgl. Dan. Vidensk. Selsk. Mat. Fys. Medd.* **35**, No. 1 (1966).  
<sup>16</sup>A. Bohr and B. R. Mottelson, *Nuclear Structure* (Benjamin, Reading, MA, 1969), Vol. 1; *Nuclear Structure* (Benjamin, Reading, MA, 1975), Vol. 2.  
<sup>17</sup>W. Nazarewicz, P. Olanders, I. Ragnarson, J. Dudek, G. A. Leander, P. Möller, and E. Ruchowska, *Nucl. Phys. A* **429**, 269 (1984).  
<sup>18</sup>A. Abbas, N. Auerbach, N. Van Giai, and L. Zamick, *Nucl. Phys. A* **367**, 189 (1981).  
<sup>19</sup>A. Sobiczewski, Z. Patyk, S. Ćwiok, and P. Rozmej, *Nucl. Phys. A* **485**, 16 (1988).  
<sup>20</sup>S. Ćwiok and W. Nazarewicz, *Nucl. Phys. A* **496**, 367 (1989).  
<sup>21</sup>W. R. Phillips, I. Ahmad, H. Emling, R. Holzmann, R. V. F. Janssens, T.-L. Khoo, and M. W. Drigert, *Phys. Rev. Lett.* **57**, 3257 (1986); see also, W. R. Phillips *et al.*, *Phys. Lett. B* **212**, 402 (1988), and references therein.  
<sup>22</sup>M. Gai, J. F. Ennis, D. A. Bromley, H. Emling, F. Azgui, E. Grosse, H. J. Wollersheim, C. Mittag, and F. Riess, *Phys. Lett. B* **215**, 242 (1988).  
<sup>23</sup>H. Mach, W. Nazarewicz, D. Kusnezov, M. Moszyński, B. Fogelberg, M. Hellström, L. Spanier, R. L. Gill, R. F. Casten, and A. Wolf, *Phys. Rev. C* **41**, R2469 (1990).